Climate-driven Habitat Changes and Refugia Dynamics for Asian Elephants in Bhutan under CMIP6 Scenarios

Wangdi[1] and Laxmi Sagar[2*]

[1]Department of Forest and Park Services, Ministry of Energy and Natural Resources, Thimphu, Bhutan, 11001

[2]Department of Forest Science, College of Natural Resources, Royal University of Bhutan, Lobesa, Punakha, 14001.

[*]Corresponding author: sagarlssagar19@gmail.com

Abstract

Bhutan maintains one of the world's highest protected areas (PA) coverage rates (52% of national territory), yet systematic assessment of these networks safeguarding its wildlife from climate change remains absent. This study modelled present-day and future habitat suitability of the Asian elephant (*Elephas maximus* Linnaeus, 1758) across Bhutan's national extent using an ensemble of four algorithms: Generalised Linear Model (GLM), Random Forest (RF), Boosted Regression Trees (BRT), and Maximum Entropy (MaxEnt). These were calibrated with 252 georeferenced presence records and 837 field-verified true absences against 17 ecologically relevant predictors. Future projections spanned 96 climate scenarios (8 General Circulation Models × 4 Shared Socioeconomic Pathways × 3 periods: 2021–2050, 2051–2080, 2071–2100) from CMIP6. All algorithms achieved high discriminatory performance, with AUC values ranging from 0.922 to 0.960 and Boyce Index from 0.964–1.000, which substantially exceeded null model expectations (all empirical $p < 0.010$). Precipitation of the warmest quarter (BIO18) was the dominant habitat driver in three of four algorithms, with driest-month precipitation (BIO14) dominant in GLM, together defining the subtropical moisture envelope critical for elephant persistence. Currently, 4,649 km² (14.1% of Bhutan) is classified as suitable habitat, concentrated in the subtropical southern belt, of which 74.1% lies outside the formal PA network. This represents a fundamental mismatch between PA placement and lowland megafauna requirements. Projected habitat change ranged from −6.1% (SSP5-8.5, 2021–2050) to +19.1% (SSP5-8.5, 2071–2100), with SSP1-2.6 and SSP5-8.5 converging to equivalent total habitat by century end despite opposite emission trajectories. Critically, 4,160 km² (12.6% of Bhutan) constitutes climate-stable core refugia, of which 53.6% lies outside the PA network. Mean human-elephant conflict risk is projected to escalate from 0.103 (present) to 0.140 under SSP5-8.5 by 2071–2100, validated against 152 observed conflict incidents. These findings suggest a looming spatial paradox where critical survival zones coincide with high-conflict hotspots. Conservation efforts must shift from static site protection to dynamic, landscape-level connectivity and the proactive management of human-elephant coexistence in climate-resilient zones. Priority interventions include expanding Bhutan's biological corridor network to encompass unprotected refugia, designating Other Effective Area-Based Conservation Measures (OECMs) on community lands in the southern belt, and scaling conflict mitigation infrastructure in this region.

Keywords: Bhutan, climate change, human–wildlife conflict, megaherbivore conservation, protected area gap

1. Introduction

The Asian elephant (*Elephas maximus* Linnaeus, 1758) is a flagship species of global conservation concern and is currently listed as Endangered on the IUCN Red List of Threatened Species (Choudhury et al., 2008). Global wild populations are estimated at 40,000–50,000 individuals, representing a decline exceeding 50% over three generations driven primarily by habitat loss, fragmentation, and escalating human–wildlife conflict (HWC) (Choudhury et al., 2008; Leimgruber et al., 2003; Sukumar, 2006). In the Eastern Himalayan region, elephant populations occupy highly heterogeneous landscapes spanning steep altitudinal and climatic gradients, where even modest shifts in precipitation seasonality or thermal regimes can substantially alter habitat connectivity and resource availability (Williams et al., 2020). Climate change therefore represents an emerging threat multiplier that amplifies existing pressures from land-use change and intensifies the spatial overlap between human settlements and elephant movement corridors (Chen et al., 2011; de Silva & Leimgruber, 2019).

Bhutan occupies a strategically critical node in the transboundary elephant landscape connecting northeastern India (Assam, Arunachal Pradesh, West Bengal) with populations in Bangladesh and represents the northernmost extent of viable lowland elephant habitat in the Eastern Himalayas (Choudhury et al., 2008). As the world's only carbon-negative country, its constitution mandates a minimum 60% national forest cover and enshrines the principle of Gross National Happiness (GNH) as the framework for national development, placing environmental conservation at the centre of policy. Accordingly, Bhutan's PA network covers 19,965 km² (52% of national area), comprising five national parks, four wildlife sanctuaries, one strict nature reserve, and nine biological corridors, among the highest PA coverage rates globally (Department of Forest and Park Services [DoFPS], 2020). Despite this exceptional governance context, Bhutan's elephant population (estimated 500–700 individuals; DoFPS, 2020) faces mounting pressures from agricultural expansion in the southern Himalayan foothills, increasing road and infrastructure development, and the progressive penetration of climate change into the montane–tropical ecotonal zone. These pressures are compounded by a structural gap in Bhutan's conservation architecture: the PA network is predominantly configured around high-elevation alpine and temperate ecosystems, leaving the subtropical southern belt, which constitutes the primary elephant habitat, chronically underrepresented in formal protection (DoFPS, 2020).

Species distribution modelling (SDM), also termed ecological niche modelling, provides a rigorous statistical framework for quantifying species–environment relationships and translating them into spatially explicit predictions of habitat suitability (Elith & Leathwick, 2009; Franklin, 2010). When coupled with climate change projections, SDMs enable prospective conservation planning by identifying areas of committed habitat loss, potential range expansion, and climate-stable refugia, defined as areas projected to remain suitable across emission scenarios (Keppel et al., 2012; Morelli et al., 2020). The application of multi-algorithm ensemble approaches, which combine predictions across algorithms to reduce model-specific uncertainty and improve predictive robustness (Araújo & New, 2007; Hao et al., 2020), has become a methodological standard in the field (Zurell et al., 2020). While SDM studies of Asian elephants have been conducted at regional (Mondal et al., 2023) or range-wide scales (Fernando et al., 2012); none have applied the full CMIP6 multi-model ensemble with verified field absence data and spatial cross-validation at national scale in Bhutan. Furthermore, no study has examined whether

Bhutan's globally exceptional PA network is actually positioned to safeguard elephant habitat under climate change.

Therefore, this study presents the first nationally comprehensive, multi-algorithm ensemble SDM for *Elephas maximus* in Bhutan, integrating true presence-absence field data, CMIP6 future climate projections, and spatially blocked cross-validation to address four conservation-oriented objectives: (1) characterise present-day habitat suitability and its key environmental drivers; (2) project habitat change and quantify associated uncertainty across 96 future climate scenarios; (3) delineate climate-stable refugia and assess their coverage within the PA network; and (4) map current and future human–elephant conflict risk hotspots. The analysis provides nationally applicable evidence base for integrated human–wildlife conflict management plan, and long-term protected area management frameworks, while also offering a methodological template applicable to other megafauna in similarly complex montane conservation landscapes.

2. Materials and Methods

2.1 Study area

The study encompassed the full national extent of Bhutan (26.7°–28.3°N, 88.8°–92.1°E; 32,973 km²), a landlinked kingdom in the Eastern Himalayas spanning an altitudinal gradient from approximately 100 m in the subtropical southern foothills to over 7,500 m in the northern alpine ranges. Bhutan's climate transitions from humid subtropical in the south where mean annual rainfall exceeds 5,000 mm in some valleys, through temperate broadleaf and conifer forests to alpine shrublands and glacial terrain in the north. The PA network includes five national parks, four wildlife sanctuaries, one strict nature reserve, and nine biological corridors (DoFPS, 2020). Elephant habitat is restricted to the subtropical southern arc, broadly below 1,500 m elevation, characterised by subtropical broadleaf forests, alluvial plains, and agricultural mosaic (DoFPS, 2020). All spatial analyses were performed in EPSG:32645 (WGS 84 / UTM Zone 45N) (Figure 1).

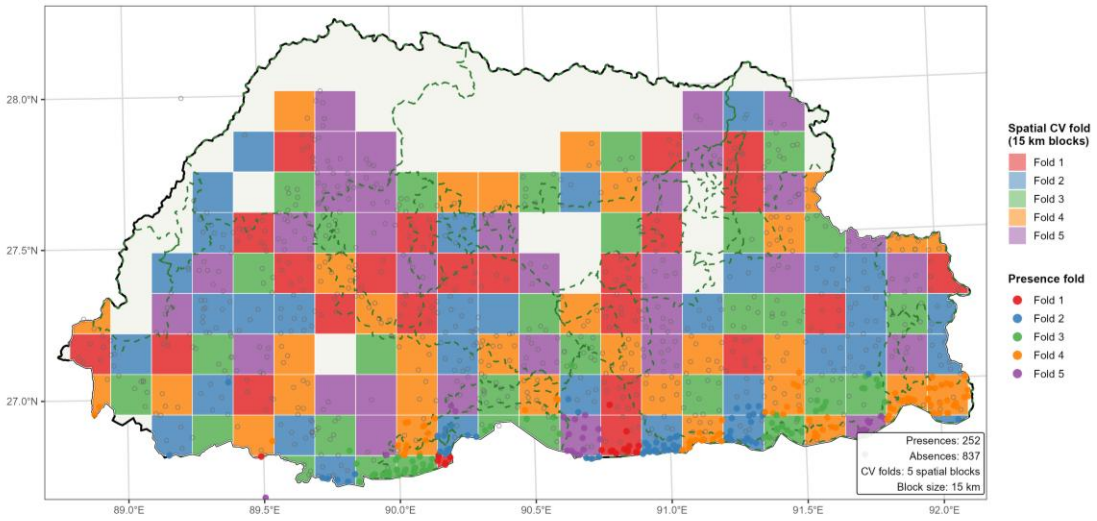

Figure 1. Study area and spatial cross-validation design for *Elephas maximus* SDM in Bhutan. Bhutan national boundary (black outline); protected area boundaries (dashed green); five-fold spatially blocked cross-validation structure (15 km blocks, coloured by fold assignment: Fold 1

red, 2 blue, 3 green, 4 orange, 5 purple). Filled circles = presence records (n = 252), coloured by fold; open circles = absence records (n = 837). Records are concentrated in the subtropical southern belt. All spatial analysis in EPSG:32645 (WGS 84 / UTM Zone 45N).

2.2 Occurrence data

Occurrence records were derived from the national elephant and tiger survey databases maintained by the Department of Forests and Park Services (DoFPS, 2020), comprising systematically deployed camera-trap stations across Bhutan. Each station was classified as a presence when the Asian Elephant (*Elephas maximus*) was detected in at least one sampling event, and as an absence when no detections were recorded over the survey period, thereby generating binary presence–absence data. Data cleaning followed a strict protocol. Coordinate validity checks were first applied to remove records with invalid geographic bounds or zero coordinates. This was followed by exact coordinate deduplication to six decimal places, conducted independently for presence and absence datasets. No pseudo-absence generation was performed, as absences were directly derived from surveyed camera-trap stations. From an initial set of 1,089 camera-trap stations, the cleaning procedure retained 252 presence stations and 837 verified absence stations, yielding a presence-to-absence ratio of 1:3.3 (Table S14; Figure S10). Additional spatial thinning was applied using a 5 km threshold to reduce spatial clustering, ensuring that retained records represent spatially independent sampling locations.

2.3 Environmental predictors

A total of 36 candidate predictor variables were compiled across four domains. The climate domain included 19 bioclimatic variables representing baseline conditions for 1986–2015 (hereafter 'present-day' throughout this study), derived from the high-resolution (250 m) CMIP6-based air temperature and precipitation grids for Bhutan developed by Dorji et al. (2025). Topographic variables included elevation (TanDEM-X 12.5 m ALOS DEM), slope, aspect, and terrain ruggedness index (TRI). To account for vegetation and land cover the annual mean Enhanced Vegetation Index (EVI; MOD13Q1, 2000–2024), annual mean Normalised Difference Vegetation Index (NDVI; MOD13Q1, 2000–2024), and a land-cover probability layer (Google Dynamic World 10 m, 2025 composite; Brown et al., 2022) was utilised. Anthropogenic and hydrological factors were represented by the Human Influence Index (HII, 2020 update; WCS/CIESIN, 2005) and Euclidean distances to major rivers, streams, water sources, settlements, protected area boundaries, and private land (cadastral boundaries). Distance to roads was excluded due to data unavailability.

Collinearity was assessed using Pearson correlation ($|r| \geq 0.85$) and Variance Inflation Factor (VIF $\geq$ 10), with predictors iteratively removed retaining those with stronger ecological justification and lower intercorrelations. Elevation was removed due to high correlation with maximum temperature ($r = -0.98$ with BIO05), as was NDVI ($r = 0.86$ with Dynamic World probability) and 13 bioclimatic variables with excessive pairwise correlations. This procedure reduced the candidate set to 17 retained predictors: BIO05 (maximum temperature of warmest month), BIO14 (precipitation of driest month), BIO15 (precipitation seasonality), BIO18 (precipitation of warmest quarter), terrain ruggedness index, slope, aspect, Human Influence Index, EVI, Dynamic World land-cover probability, land-cover class, and Euclidean distances to major rivers, streams, water sources, settlements, protected areas, and private land (Table S1; Figure S6; Appendix S2).

2.4 Species distribution modelling

A four-algorithm ensemble SDM was implemented, following the multi-algorithm comparative framework of Elith et al. (2006), comprising:

1. **Generalised Linear Model (GLM)**: Binomial family with a logit link; predictor selection via forward stepwise AIC minimisation.
2. **Random Forest (RF; Breiman, 2001)**: Implemented in the ranger package; 1,000 trees, *mtry* = 4 ($\lfloor\sqrt{17}\rfloor$), minimum node size = 1; variable importance via permutation.
3. **Boosted Regression Trees (BRT; Friedman, 2001; Elith et al., 2008)**: Implemented in gbm; 1,000 trees, interaction depth = 3, learning rate = 0.01, bag fraction = 0.5; best iteration selected by out-of-bag stopping; variable importance via relative influence.
4. **Maximum Entropy (MaxEnt; Phillips et al., 2006; 2017):** Feature types: linear, quadratic, hinge, and product; regularisation multiplier $\beta = 1.5$, selected as appropriate for small sample sizes (Merow et al., 2013). Full algorithm hyperparameters and software versions are given in Table S4.

All models were calibrated using five-fold spatially blocked cross-validation (15 km block size; Roberts et al., 2017; Valavi et al., 2019), with fold assignments minimising spatial autocorrelation between training and evaluation sets (seed = 123458). Out-of-fold (OOF) predictions were aggregated to generate evaluation datasets spanning the full geographic extent. The ensemble prediction was computed as an AUC-weighted mean across algorithms, restricted to algorithms exceeding a minimum AUC of 0.65 (all four algorithms qualified). Optimal binary classification thresholds were derived by maximising the true skill statistic (TSS) on OOF predictions; because MaxEnt OOF probabilities fell outside the standard [0,1] range, a TSS-maximising threshold could not be computed for that algorithm and its threshold was instead derived from the full-model predictions (sensitivity to alternative cutoffs: Table S6; Figure S7). All stochastic operations were seeded for reproducibility (global seed = 123456; per-module seeds documented in the project configuration).

2.5 Model evaluation

Model performance was assessed using six complementary metrics on OOF predictions:

- **AUC** (area under the Receiver Operating Characteristics curve): overall discriminatory ability, which is independent of the threshold
- **TSS** (True Skill Statistic = sensitivity + specificity − 1): threshold-dependent performance that accounts for both error types (reported for GLM, RF, and BRT; not computed for MaxEnt)
- **Boyce Index** (Hirzel et al., 2006): measures continuous suitability ranking and is independent of the threshold
- **Brier Score**: represents the mean squared error of probabilistic predictions (lower is values indicate superior performance)
- **Calibration Slope**: calculated via logistic regression of the observed outcome on the predicted probability, where a slope = 1.0 indicates perfect calibration
- **Moran's *I***: measures the spatial autocorrelation of OOF residuals; any deviation from zero indicates residual spatial structure not captured by the model

Statistical significance was assessed by comparing observed AUC against null distributions from 99 label-permuted null models (empirical $p < 0.010$ constitutes rejection of the null hypothesis). No ensemble-level OOF evaluation was computed, as this would require withheld predictions from all four algorithms simultaneously on the same fold structure. This limitation is acknowledged. Confusion matrices (including True Positives [TP], True Negatives [TN], False Positives [FP], False Negatives [FN], sensitivity, specificity, Positive Predictive Value [PPV], Negative Predictive Value [NPV]) were derived at the TSS-maximising ensemble threshold (0.174).

2.6 Future climate projections

Future habitat suitability was projected onto 96 climate scenarios from the CMIP6 multi-model ensemble: 8 General Circulation Models (GCMs) × 4 Shared Socioeconomic Pathways (SSP1-2.6, SSP2-4.5, SSP3-7.0, and SSP5-8.5) × 3 time periods (2021–2050, 2051–2080, and 2071–2100). GCMs comprised: ACCESS-CM2, CNRM-CM6-1, CNRM-ESM2-1, INM-CM4-8, INM-CM5-0, MIROC6, MPI-ESM1-2-LR, and MRI-ESM2-0, representing diverse climate sensitivities and model families (Sanderson et al., 2015). All 96 scenarios were completed successfully.

The reliability of the GCMs was ranked by a composite score combining intra-algorithm prediction standard deviation (SD) and deviation from the multi-model ensemble mean (Appendix S3; Table S8; Figure S13). Individual GCM habitat area trajectories are tabulated in Table S10 and shown in Figure S14. INM-CM5-0 ranked first (composite score = 0.840), followed by CNRM-CM6-1 (0.804) and MIROC6 (0.796). ACCESS-CM2 (0.356) and MRI-ESM2-0 (0.000) received the lowest scores and contributed negligible weight to the AUC-weighted ensemble. Climate analogue extrapolation risk was quantified via the Multivariate Environmental Surface (MESS; Elith et al., 2010); the mean extrapolation fraction across all 96 scenarios was 0.0011 (0.11% of pixels), confirming minimal novel-climate risk (Table S15; Figure S8; Figure S21). Gain, loss, and persistence of binary habitat relative to the present-day baseline were computed for each scenario. Ensemble uncertainty was quantified as the inter-GCM standard deviation of continuous suitability predictions. Niche similarity between present and future projections was characterised using Schoener's *D* (range: 0.791–0.867) and Hellinger's *I* (0.968–0.985), confirming high climatic coherence across scenarios (Table S17).

2.7 Climate refugia identification

Climate refugia defined as areas maintaining habitat suitability regardless of emission scenario, were identified by computing a stability count raster recording, that recorded, for each pixel, the number of the 12 future SSP × time period combinations in which the ensemble prediction exceeded the binary threshold. Pixels were classified into five stability classes: (1) never suitable (0 of 12 scenarios); (2) low stability (1–3 scenarios; <25%); (3) moderate stability (4–6; 25–50%); (4) high stability (7–9; 50–75%); and (5) core refugia (10–12; >75%). Core refugia, which are suitable under all or nearly all scenarios, represent the most climate-resilient nodes of elephant habitat. Protected coverage of each stability class was assessed by overlaying these results with the national PA boundary.

2.8 Human–elephant conflict risk mapping

Present-day human–elephant conflict (HEC) risk was operationalised as the spatial product of ensemble habitat suitability (representing the likelihood of elephant presence) and the Human

Influence Index (HII, representing exposure to agriculture, settlements, and infrastructure). The resulting conflict risk index was classified into four risk zones: (1) low (≤0.040); (2) moderate (0.040–0.069); (3) high (0.069–0.164); and (4) very high (>0.164). Spatial predictions were validated against 152 confirmed Human Elephant Conflict (HEC) incident locations (derived from DoFPS conflict records, 2015–2023) that recorded crop damage, property damage, and human casualties in the southern Dzongkhags (districts). Future conflict risk was projected for all 12 SSP × time period combinations by applying the conflict risk formula to each future suitability surface, thereby yielding a time-series of mean conflict risk indices.

2.9 Reproducibility

All analyses were implemented in R v4.4.0 (R Core Team, 2024). Complete code, configuration, and execution logs are archived under run ID RUN_20260326_104659_b990 (pipeline version 3.0-bhutan-national). Compliance with Overview, Data, Model, Analysis, and Prediction (ODMAP) protocol (Zurell et al., 2020) is documented in Supplementary Appendix S1 (Table S16).

3. Results

3.1 Model performance

All four algorithms substantially outperformed label-permuted null models (empirical $p < 0.010$) and exceeded all pre-specified performance thresholds (AUC ≥ 0.65, TSS ≥ 0.30, Boyce Index ≥ 0.10, Brier Score ≤ 0.25; Table 1; Figure S2; Figure S4). MaxEnt achieved the highest discriminatory performance (AUC = 0.960) and the lowest Brier Score (0.080), while RF attained the highest sensitivity (0.960) and negative predictive value (NPV = 0.986). The GLM performed at the lower bound of the ensemble but remained excellent (AUC = 0.922). Calibration slopes ranged from 0.846 (GLM; indicating slight under-prediction) to 1.292 (RF) and 1.279 (BRT), indicating modest over-dispersion in tree-based methods, while MaxEnt showed near-perfect calibration (slope = 0.935) (Figure S3). Spatial autocorrelation in OOF residuals (Moran's I = 0.099–0.217) was uniformly low, confirming that spatially blocked cross-validation effectively reduced residual spatial structure (Roberts et al., 2017) (Figure S20). Performance was consistent across the five folds (AUC range: 0.877–0.989; Table S5a; Table S5b; Figure S5), though Fold 1 contained only 19 presence records (balance ratio = 0.12), yielding wider performance intervals in that instance.

Table 1. Model performance metrics for each algorithm evaluated on out-of-fold (OOF) predictions using five-fold spatially blocked cross-validation (block size = 15 km; seed = 123458).

Algorithm	AUC	TSS	Boyce Index	Brier Score	Calib. Slope	Moran's I	Threshold	Sensitivity	Specificity	PPV	NPV
GLM	0.922	0.750	0.988	0.096	0.846	0.217	0.162	0.897	0.824	0.606	0.964

Algorithm	AUC	TSS	Boyce Index	Brier Score	Calib. Slope	Moran's I	Threshold	Sensitivity	Specificity	PPV	NPV
RF	0.948	0.819	0.988	0.081	1.292	0.154	0.218	**0.960**	0.842	0.647	**0.986**
BRT	0.943	0.795	**1.000**	0.086	1.279	0.201	0.179	0.921	0.842	0.637	0.972
MaxEnt	**0.960**	—†	0.964	**0.080**	**0.935**	**0.099**	0.140‡	0.938	0.837	0.632	0.978

AUC = area under the ROC curve; TSS = true skill statistic (sensitivity + specificity − 1); Boyce Index = continuous Boyce index; Brier Score (lower = better); Calibration Slope (1.0 = perfect); Moran's I of OOF residuals (0 = no autocorrelation); PPV = positive predictive value; NPV = negative predictive value. Bold = best per column. All algorithms significantly outperform 99-permutation null models (empirical $p < 0.010$). †MaxEnt TSS not computed: OOF probabilities outside standard [0,1] range. ‡MaxEnt threshold derived from full-model predictions. No ensemble-level OOF evaluation was computed.

3.2 Environmental drivers of habitat suitability

Precipitation of the warmest quarter (BIO18) was the highest-ranked predictor in three of four algorithms (RF: normalised importance = 100%; BRT: 100%; MaxEnt: 100%), establishing it as the primary determinant of elephant habitat suitability in Bhutan (Table S3; Figure 2). Precipitation of the driest month (BIO14) ranked first in the GLM (100%) and second in RF (64.9%), confirming its importance as the complementary dry-season constraint. Together, BIO18 and BIO14 define the subtropical moisture envelope; BIO18 governs monsoon-season forage productivity and fat accumulation, while BIO14 governing dry-season water point persistence and lean-season ranging constraints (Sukumar, 1989; de Silva & Leimgruber, 2019). Maximum temperature of the warmest month (BIO05; importance = 10–44% across algorithms), terrain ruggedness index (TRI; 14–27%), and distance to protected areas (15–27%) were consistently ranked in the top five across all algorithms.

Response curves revealed that suitable habitat was associated with reliable dry-season precipitation (BIO14 > 10 mm month^{-1}), high monsoon-season rainfall (BIO18 > 1,500 mm), warm maximum temperatures (BIO05 > 26°C), and moderate topographic ruggedness (full marginal response curves for all 17 predictors: Figure S9). Presence stations showed significantly higher values for BIO18 (mean ± SD: 2,085.8 ± 676.9 mm vs. 1,032.5 ± 500.7 mm at background stations; Cohen's d = +1.77) and BIO14 (12.5 ± 4.5 vs. 6.1 ± 3.8 mm; d = +1.53), confirming strong climate-mediated habitat filtering (Table S2; Figure 2). In MaxEnt, slope received anomalously high importance (29.4%) relative to GLM (0.1%), RF (7.1%), and BRT (3.3%), likely an artefact of MaxEnt's feature-type interactions with lowland flat-terrain variables.

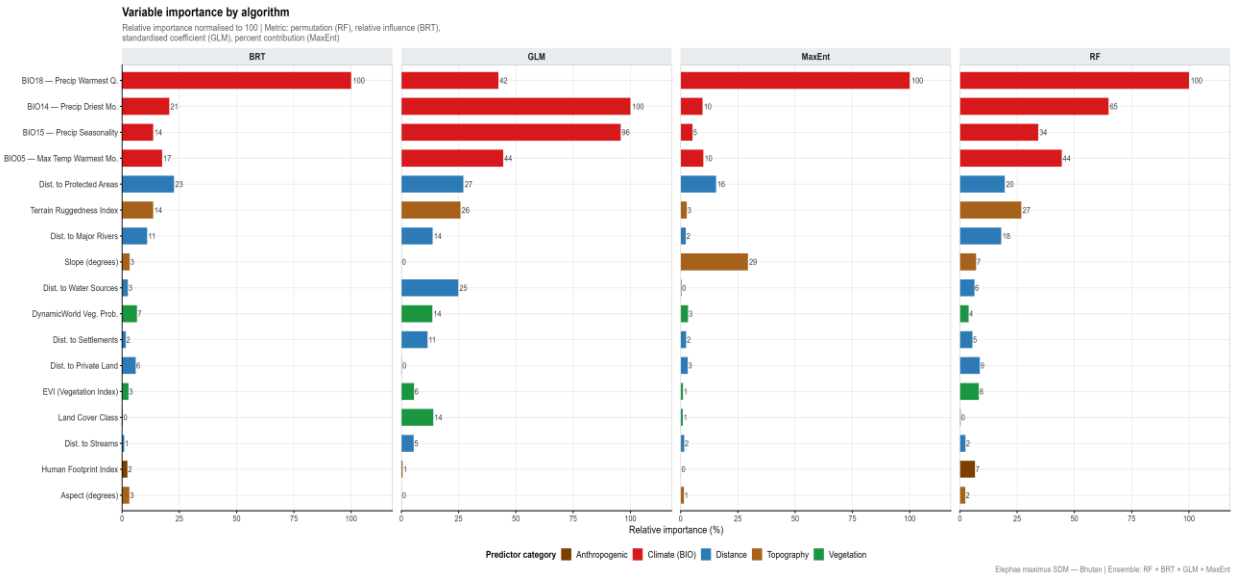

Figure 2. Environmental drivers of *Elephas maximus* habitat suitability in Bhutan. Normalised variable importance across four algorithms (GLM: coefficient t-statistic; RF: permutation importance; BRT: relative influence; MaxEnt: percent contribution), values normalised so the maximum per algorithm = 100%. BIO18 (precipitation of warmest quarter) ranks first in RF, BRT, and MaxEnt; BIO14 (precipitation of driest month) ranks first in GLM. Predictor categories: blue = climate, green = topography, orange = vegetation/land cover, red = anthropogenic/distance.

3.3 Present-day habitat suitability and protected area coverage

The ensemble model (AUC-weighted mean, threshold = 0.174) identified 4,649 km² (14.1% of Bhutan) as currently suitable habitat for Asian Elephants (Table 3; Figure 3; per-algorithm maps: Figure S1). Suitable habitat is concentrated in a contiguous southern arc spanning Samtse and Chhukha Dzongkhags in the west through Dagana, Tsirang, Sarpang, and Zhemgang to Pemagatshel and Samdrup Jongkhar in the east (Figure 3). The five Dzongkhags with the highest habitat coverage were Samdrup Jongkhar (69.4% of district area; 1,301 km²), Pemagatshel (58.8%; 602 km²), Sarpang (58.4%; 967 km²), Zhemgang (32.5%; 779 km²), and Dagana (26.4%; 447 km²; Table S13).

Of the 4,649 km² of suitable habitat, 1,207 km² (25.9%) lies within the formal PA network, representing 6.1% of total PA area, while 3,442 km² (74.1%) lies outside formal protection (Table 3). Biological Corridor 5 (100% of unit area suitable; 219 km²; mean suitability = 0.743), Phibsoo Wildlife Sanctuary (100%; 298 km²; mean = 0.720), and Jomotsangkha Wildlife Sanctuary (100%; 372 km²; mean = 0.635) were entirely suitable, whereas high-elevation national parks contributed negligible suitable area (Table S7). Royal Manas National Park contributed the largest single PA area of suitable habitat (77.5% suitable; 837 km²).

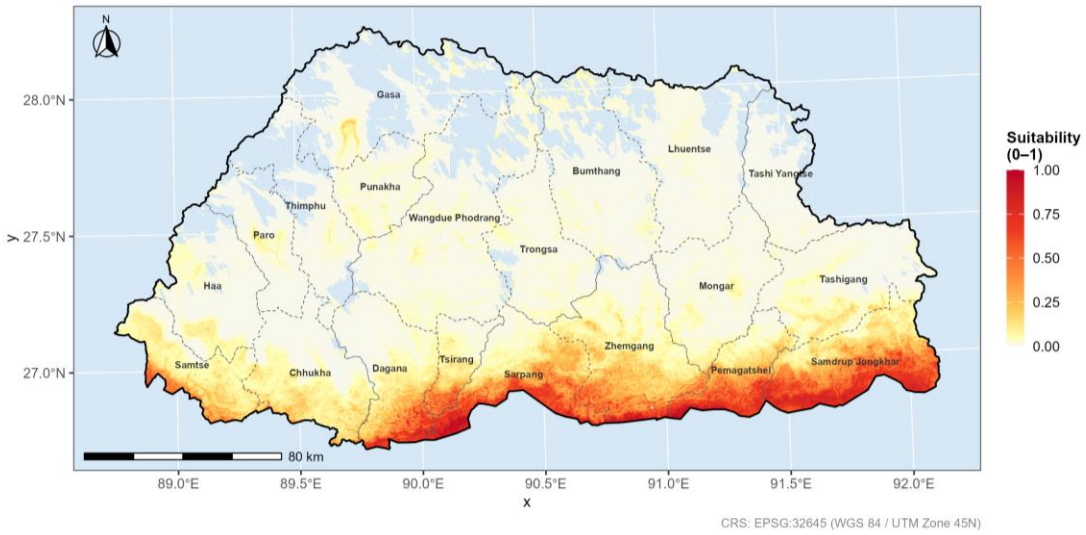

Figure 3. Present-day habitat suitability of *Elephas maximus* in Bhutan. Ensemble AUC-weighted mean suitability (GLM + RF + BRT + MaxEnt; 1986–2015 climate baseline; EPSG:32645). High suitability (red–yellow) is concentrated in the subtropical southern belt below ~1,500 m. The PA network boundary is overlaid (black outline). Of 4,649 km² of suitable habitat (threshold = 0.174), 74.1% lies outside the formal PA network.

3.4 Future habitat trajectories

Future habitat area showed scenario-dependent dynamics characterised by near-term contraction under high-warming pathways followed by general expansion as climate shifts open submontane zones (Table 2; Figure. 4; full suitability maps: Figure S15; change maps: Figure S16). Under SSP5-8.5, habitat contracted most sharply in the near term (4,364 km²; −6.1% relative to the 4,649 km² present-day baseline by 2021–2050), driven by intensified thermal stress at low-elevation margins, before recovering to 5,539 km² (+19.1%) by 2071–2100 as warming expands the suitable thermal envelope into the submontane zone. SSP1-2.6 showed modest near-term contraction (4,608 km²; −0.9% by 2021–2050) followed by progressive expansion to 5,528 km² (+18.9%) by 2071–2100. Strikingly, SSP1-2.6 and SSP5-8.5 converge to nearly identical total habitat area at century end (+18.9% and +19.1%, respectively), despite representing the most divergent emission pathways. SSP3-7.0 showed the most conservative trajectory, returning to near-present-day conditions by 2071–2100 (+0.9%; 4,690 km²).

Habitat persistence dominated under all scenarios, exceeding 4,216 km² even at maximum contraction (Table 2). New habitat gain areas were concentrated at higher elevations (approximately 800–1,800 m) in the submontane zone, while loss areas were concentrated at the southern thermal extreme (Fig. S17). Inter-GCM uncertainty was highest under SSP5-8.5 by 2071–2100 (mean GCM SD = 0.042; 11.3% of pixels flagged as high uncertainty; Table S9; Table S10; Figure S11; Figure S12; Figure S18). Niche similarity between present and future conditions was high across all scenarios (Schoener's D = 0.791–0.867; Hellinger's I = 0.968–0.985), confirming that projections remain within the training climate envelope.

Table 2. Projected habitat area, net change, gain, loss, and persistence for *Elephas maximus* in Bhutan under four Shared Socioeconomic Pathways and three time periods.

SSP	Period	Total area (km²)	Net change (%)	Gain (km²)	Loss (km²)	Persistence (km²)	GCM SD (mean)
SSP1-2.6	2021–2050	4,608	−0.9%	255	308	4,354	0.022
SSP1-2.6	2051–2080	5,133	+10.4%	556	85	4,577	0.024
SSP1-2.6	2071–2100	5,528	+18.9%	905	39	4,623	0.031
SSP2-4.5	2021–2050	4,681	+0.7%	297	279	4,383	0.021
SSP2-4.5	2051–2080	4,879	+4.9%	443	226	4,436	0.022
SSP2-4.5	2071–2100	5,413	+16.4%	825	73	4,589	0.037
SSP3-7.0	2021–2050	4,868	+4.7%	541	335	4,327	0.017
SSP3-7.0	2051–2080	4,795	+3.1%	426	293	4,369	0.027
SSP3-7.0	2071–2100	4,690	+0.9%	378	350	4,312	0.028
SSP5-8.5	2021–2050	4,364	**−6.1%**	148	446	4,216	0.016
SSP5-8.5	2051–2080	5,012	+7.8%	525	175	4,487	0.033
SSP5-8.5	2071–2100	5,539	**+19.1%**	946	69	4,593	0.042

Net change relative to present-day baseline (4,649 km²; threshold = 0.174). GCM SD = mean inter-GCM standard deviation of continuous suitability across 8 GCMs. Bold = extremes of range.

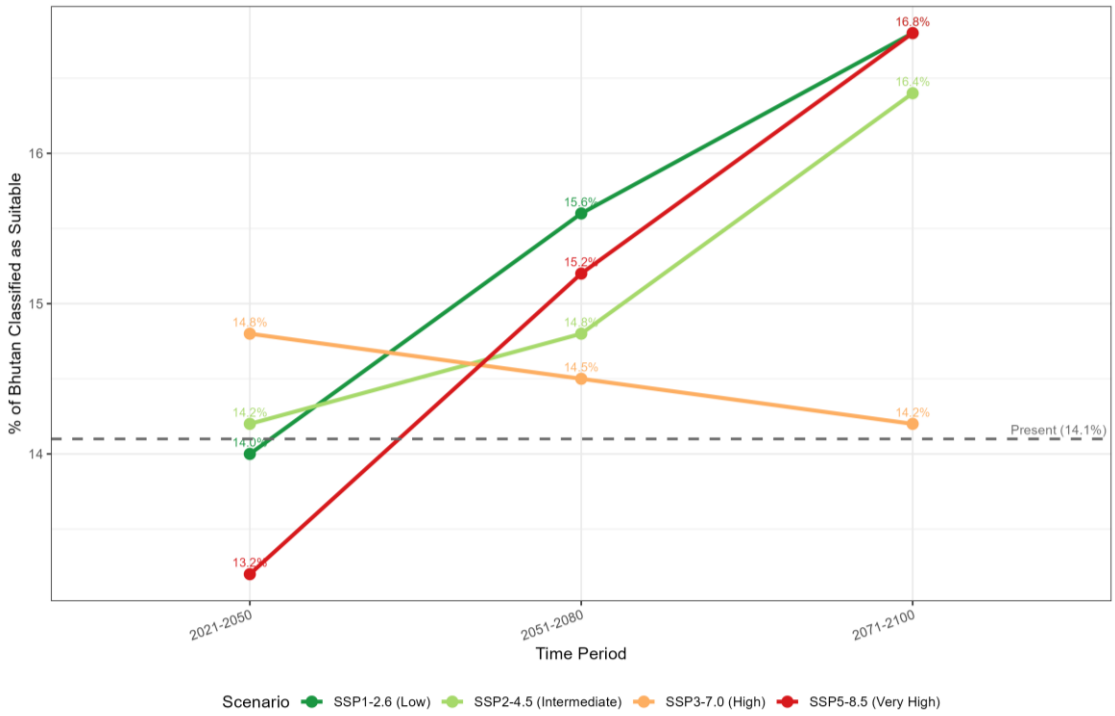

Figure 4. Future habitat trajectories for *Elephas maximus* in Bhutan across four Shared Socioeconomic Pathways (2021–2100). Lines represents the GCM-mean ensemble habitat area (8 GCMs weighted by composite reliability score); shading indicates ±1 SD across GCMs. The horizontal dashed line denotes present-day baseline (4,649 km²; 14.1% of Bhutan). Note convergence of SSP1-2.6 and SSP5-8.5 by 2071–2100 (+18.9% and +19.1%, respectively) and the steepest near-term contraction occurring under SSP5-8.5 (−6.1% by 2021–2050).

3.5 Climate refugia

Stability analysis across all 12 future SSP × period scenarios identified 4,160 km² (12.6% of Bhutan) as core refugia, defined as habitat maintaining suitability across all 12 scenarios (Table 3; Table S18; Figure 5). An additional 196 km² qualified as high-stability habitat (suitable in 10–11 of 12 scenarios), yielding a combined high-resilient area of 4,356 km² (13.2%). The spatial distribution of core refugia closely mirrors present-day suitability, concentrated in the subtropical southern belt (Figure 5). Protected coverage of core refugia was 46.4% (approximately 1,930 km²), with the remaining 53.6% (approximately 2,230 km²) situated on unprotected lands (Table 3). The highest-refugia PA units, comprising Biological Corridor 5, Phibsoo Wildlife Sanctuary, and Jomotsangkha Wildlife Sanctuary, were identical to the highest-suitability PAs under present-day conditions, indicating that these three units anchor the long-term persistence of elephant populations in Bhutan regardless of the emission scenario (Figure 5).

Table 3. Present-day habitat suitability and climate refugia: area, coverage of Bhutan, and protected area status.

Category	Definition	Area (km²)	% of Bhutan	Inside PAs (km²)	% in PAs	Outside PAs (km²)	% outside PAs

Category	Definition	Area (km²)	% of Bhutan	Inside PAs (km²)	% in PAs	Outside PAs (km²)	% outside PAs
Present suitable habitat	Ensemble suitability ≥ 0.174	4,649	14.1%	1,207	25.9%	3,442	74.1%
Core refugia	Suitable in all 12 future scenarios	4,160	12.6%	1,930	46.4%	2,230	53.6%
High-stability refugia	Suitable in ≥10 of 12 scenarios	4,356	13.2%	1,977	45.4%	2,379	54.6%

Present PA network = 19,965 km² (52% of Bhutan). 12 future scenarios = 4 SSPs × 3 time periods (2021–2050, 2051–2080, 2071–2100). Ensemble threshold = 0.174 (TSS-maximising).

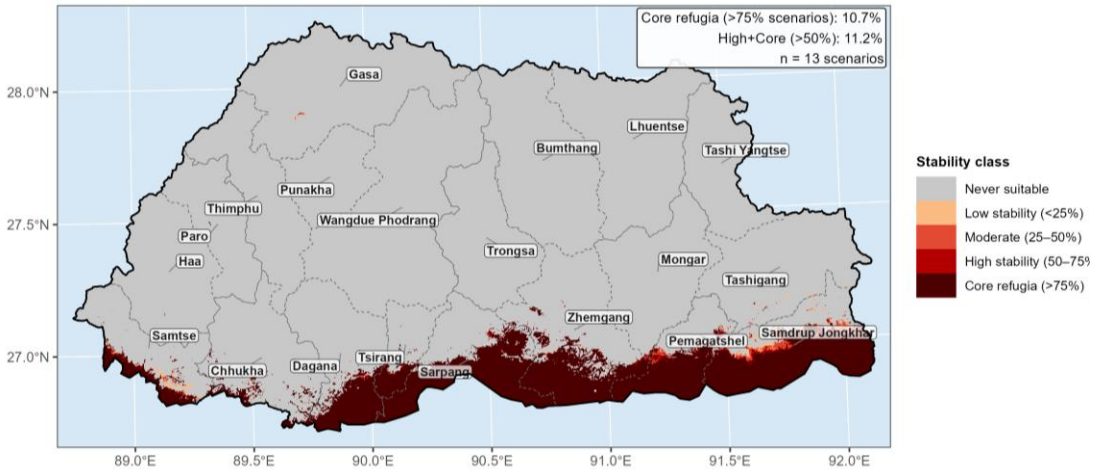

Figure 5. Climate refugia stability classification for *Elephas maximus* in Bhutan. Each 250 m pixel is classified by the number of future climate scenarios (out of 12: 4 SSPs × 3 periods) in which ensemble habitat suitability exceeds the decision threshold (0.174). Core refugia (dark red, all 12 scenarios) cover 4,160 km² (12.6% of Bhutan); 46.4% of core refugia lie within the formal PA network. Inset annotation shows stability class statistics. Source: figure_s18_refugia.png.

3.6 Human–elephant conflict risk — present and future

Present-day spatial risk mapping classified 35% of Bhutan (11,541 km²) as high or very high HEC risk (high: 6,595 km²; very high: 4,946 km²; Table S11; Figure 6). Observed HEC incidents (*n* = 152 confirmed events, 2015–2023) showed strong spatial clustering in high- and very-high-risk zones, validating the predictive accuracy of the conflict index. Incident types comprised crop damage (~60%), property damage (~25%), and human casualties (~15%), concentrated in Samdrup Jongkhar, Pemagatshel, and Sarpang, which are the same Dzongkhags with the highest habitat suitability scores.

Future conflict risk showed monotonic escalation across all SSPs and periods (Figure S19; Table S12). Under SSP1-2.6, mean risk reached 0.127 by 2071–2100 (from a baseline of 0.103); under SSP5-8.5, it reached 0.140, representing a 35.9% increase relative to the present. A non-linear inversion emerged at the end of the century: mean risk under SSP2-4.5 (0.132) exceeded that of

SSP3-7.0 (0.129) despite the former having lower radiative forcing, suggesting that precipitation redistribution under intermediate warming may increase HEC exposure via pathways beyond the direct suitability signal. Spatial coincidence between core refugia and high-conflict zones defines the fundamental conservation paradox of this study.

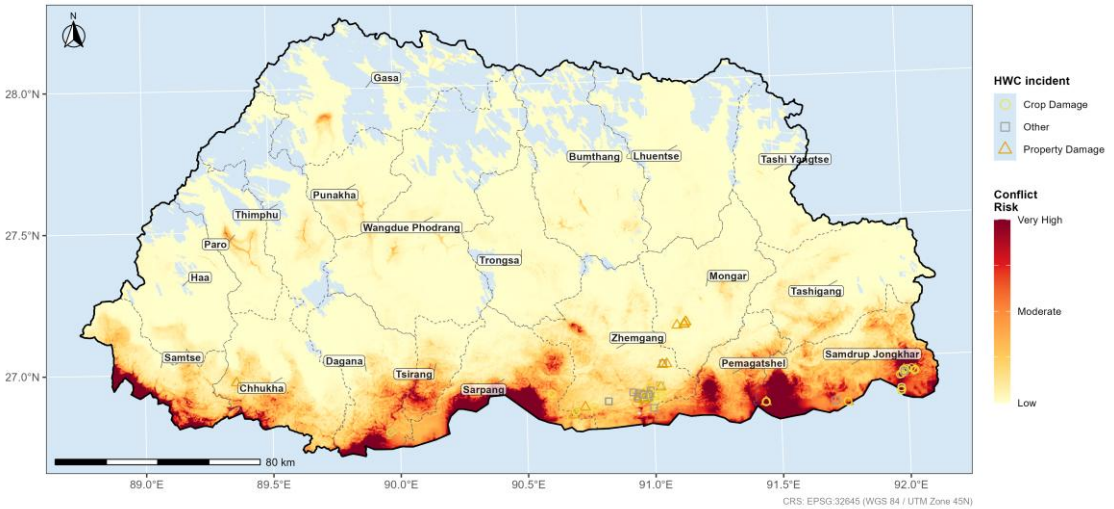

Figure 6. Present-day spatial distribution HEC risk. Risk index = ensemble habitat suitability × Human Influence Index. Risk classes: low (≤0.040), moderate (0.040–0.069), high (0.069–0.164), very high (>0.164). Confirmed HEC incident locations (*n* = 152, 2015–2023; DoFPS) are overlaid as black points, validating the conflict risk predictions. High or very high-risk zones cover 35% of Bhutan (11,541 km²). Incidents cluster in Samdrup Jongkhar, Pemagatshel, and Sarpang, which are the same Dzongkhags anchoring core refugia.

4. Discussion

4.1 The subtropical moisture envelope as the primary habitat determinant

The results demonstrate that the precipitation regime, specifically the amplitude of the monsoon peak (BIO18) and the severity of the dry-season minimum (BIO14), is the primary determinant of Asian Elephant habitat suitability in Bhutan, with BIO18 ranked first in three of four algorithms. This finding is ecologically coherent; monsoon-season rainfall (BIO18) drives peak forage productivity, enabling the fat accumulation and body condition maintenance critical for reproductive success and calf survival in Asian elephants (Sukumar, 1989; Campos-Arceiz & Blake, 2011). Dry-season precipitation (BIO14) governs the persistence of water points and patchily distributed riparian vegetation that elephants depend upon during the November–April lean season, effectively constraining the southern boundary of the viable year-round range (de Silva & Leimgruber, 2019). Together, BIO18 and BIO14 define a subtropical moisture envelope, within which elephant habitat in Bhutan is embedded, that is warm enough for monsoon productivity (BIO05 > 26°C) but reliably watered throughout the year (BIO14 > 10 mm month^{-1}).

However, the present findings contrast with Mondal et al. (2023), who found temperature variables dominant in sub-Himalayan Bengal (India), reflecting the lower elevational range and more temperature-limited habitat at the foothills of the Ganges plain. The Bhutan context, a montane landscape where temperature varies continuously along elevation, may amplify the precipitation signal by restricting accessible elephant habitat to a narrow thermal band in which

precipitation variability, rather than temperature per se, determines habitat quality. The low importance of human footprint at the national scale (importance 0.1–6.6% across), despite known elephant sensitivity to anthropogenic pressure (Barua et al., 2013), likely reflects the relatively intact landscape nature of southern Bhutan rather than species insensitivity. The unavailability of a roads layer for Bhutan means that one component of the human accessibility gradient could not be captured, representing a data gap that future studies should address.

The detection of unusually high slope importance in MaxEnt (29.4% vs. <8% in other algorithms) warrants a methodological note. MaxEnt's feature-type interactions (linear, quadratic, hinge, product) can generate complex implicit variable combinations. In low-slope, lowland terrain, which constitutes the primary elephant zones, slope co-varies with terrain accessibility and agricultural development in ways not captured by the other algorithms through single predictor importance scores. This pattern is therefore not interpreted as an independent biological signal.

4.2 The protected area coverage paradox

The finding that 74.1% of elephant habitat lies outside the formal PA network constitutes a fundamental conservation challenge, reflecting a structural feature of how Bhutan's PA system was historically configured rather than an incidental gap. National parks and wildlife sanctuaries in Bhutan were predominantly established to protect high-elevation temperate, alpine, and nival ecosystems, reflecting a global pattern of PA placement bias towards remote, low-opportunity-cost terrain (Joppa & Pfaff, 2009; Venter et al., 2018). This placement strategy optimises forest cover metrics and carbon accounting but systematically underprotects lowland megafauna whose ranges coincide with productive agricultural zones (Fernando et al., 2012). Bhutan's biological corridors provide partial mitigation, with Biological Corridor 5 and Jomotsangkha Wildlife Sanctuary entirely within suitable habitat, but their combined suitable area (590 km²) represents only 12.7% of total suitable habitat, insufficient to encompass the unprotected southern belt.

This finding mirrors broader Asian elephant conservation patterns documented across India (Choudhury et al., 2008; Mondal et al., 2023), Sri Lanka (Fernando et al., 2012), and Myanmar, where the majority of suitable habitat occurs in multiple-use landscapes outside strict protection. Under GBF Target 3 (30×30), there is an opportunity to designate Other Effective Area-Based Conservation Measures (OECMs) on community forests, private land, and agricultural mosaic in the southern belt, where 37.1% of non-PA land supports suitable elephant habitat.

For Bhutan, specifically, however this gap represents not merely a mapping problem but a governance challenge. Southern Dzongkhages including Samdrup Jongkhar, Pemagatshel, and Sarpang, where elephant habitat is most concentrated, are also the zones of highest agricultural productivity and population growth (Citation). Any landscape-level conservation strategy here must therefore negotiate between the rights and livelihoods of farming communities and the habitat requirements of a protected species. The 2,261 km² of private cadastral land with non-negligible mean suitability (0.102) is not simply a conservation opportunity, it represents a political negotiation that OECMs under GBF Target 3 must be designed to facilitate, not bypass..

4.3 Climate resilience, refugia, and the convergence paradox

The most counterintuitive finding of this study is the convergence of SSP1-2.6 and SSP5-8.5 to near-identical total elephant habitat by 2071–2100 (+18.9% and +19.1%, respectively), despite representing the most divergent emission pathways available in CMIP6. This convergence carries a critical but uncomfortable implication for conservation policy: the long-term total area

of elephant habitat in Bhutan appears largely insensitive to the level of global climate mitigation effort. However, mitigation strongly influences the near-term trajectory. Under SSP5-8.5, habitat is projected to contract by 6.1% by 2050, a decline largely avoided under SSP1-2.6. For a species with slow reproductive rates and long generation times, a 30-year squeeze on available habitat is not merely a temporary inconvenience; it represents a potential population bottleneck. The aggregate stability masks important spatial dynamics: core habitat in the lowland subtropical belt persists robustly under all scenarios (persistence area 4,216–4,623 km²), while range margins shift in response to the thermal envelope. The mechanism driving long-term gains, specifically thermally driven expansion into the submontane zone as warming elevates the lower thermal limit of suitable climate, is consistent with upslope range shifts documented across Himalayan taxa (Chen et al., 2011; Telwala et al., 2013). Whether elephants can track such shifts depends critically on landscape connectivity and anthropogenic land-use barriers in the 800–1,800 m elevational zone, which is already heavily cultivated across much of southern Bhutan.

The convergence of SSP1-2.6 and SSP5-8.5 to near-identical total habitat by 2071–2100 (+18.9% and +19.1%, respectively) reveals a counter-intuitive dynamic: aggressive mitigation does not substantially change the long-term total area of elephant habitat in Bhutan, because the thermal expansion of the submontane envelope is largely committed by current climate trajectories (Matthews & Caldeira, 2008). What mitigation does change is the near-term trajectory: SSP5-8.5 delivers the steepest near-term contraction (−6.1% by 2050), increasing population pressure on remaining refugia during the critical 2021–2050 window. Core refugia (4,160 km², 46.4% protected) represent the most actionable output of this analysis, as these are areas where habitat suitability is guaranteed under any future emission pathway and where conservation investment therefore carries the highest probability of long-term return. That 53.6% of these areas remain unprotected constitutes a critical policy gap.

4.4 The climate–conflict nexus

The projected escalation of mean conflict risk from 0.103 (present) to 0.140 under SSP5-8.5 by 2071–2100 represents a 35.9% increase in the spatial overlap of elephant presence likelihood and human exposure. This is a trajectory directly relevant to communities in Samdrup Jongkhar, Pemagatshel, and Sarpang, where 152 confirmed HEC events between 2015 and 2023 were already concentrated in high- and very-high-risk zones. The non-linear inversion in which SSP2-4.5 yields marginally higher conflict risk than SSP3-7.0 at the end of the century (0.132 vs. 0.129) suggests that conflict escalation is not a simple function of overall warming. Rather, it indicates that precipitation dynamics under intermediate scenarios may create localised habitat shifts that are not captured by aggregate metrics.

The spatial coincidence between core refugia and high-conflict zones defines the central conservation paradox of this study: the areas where elephants are most likely to persist long-term are also the areas where human exposure is highest. Effective strategies in Bhutan should prioritise early warning systems linked to elephant tracking programmes, solar-powered electric fencing along field perimeters in the highest-conflict Dzongkhags, rapid community response mechanisms for incident reporting, and crop insurance or compensation schemes that maintain community tolerance for elephant presence (Wangchuk, 2004; Wang & Macdonald, 2006; Barua et al., 2013). Crucially, these interventions must be designed for long-term escalation rather than the present-day risk baseline.

In Bhutan's governance context, where the Gross National Happiness framework formally requires balancing environmental conservation with community wellbeing, the projected escalation of conflict creates a structurally difficult trade-off. Samdrup Jongkhar, Pemagatshel, and Sarpang, the three Dzongkhags that anchor both core refugia and the highest conflict risk, are also among the most economically marginal districts in the country, where crop damage from elephants can represent a disproportionate share of household income. Conflict mitigation infrastructure in these districts therefore cannot be treated as a technical add-on to conservation planning; rather, it is a prerequisite for maintaining the community tolerance on which any long-term coexistence strategy depends.

4.5 Methodological considerations

Several strengths distinguish this study from previous regional elephant SDMs. The use of verified true presence-absence field data, rather than pseudo-absences generated from background sampling, provides a more direct characterisation of the occupied versus unoccupied landscape and eliminates potential biases introduced by background selection procedures (Hirzel & Le Lay, 2008; Guisan et al., 2002). The CMIP6 eight-GCM ensemble, with explicit GCM reliability weighting and full-range uncertainty quantification, represents a substantial advance over single-GCM or two-GCM future scenarios common in regional SDM studies. Spatial block cross-validation (Valavi et al., 2019; Roberts et al., 2017) ensures that evaluation metrics reflect geographic transferability rather than spatial autocorrelation inflation, producing conservative but more realistic performance estimates.

However, several limitations of the study should be noted. The presence dataset exhibits a positive spatial bias, with 63.5% of records from inside PA, which may inflate apparent suitability inside PAs and consequently, the importance of dist_to_protected_areas as a predictor. The absence of a roads layer introduces a gap in the human accessibility gradient. The SDM framework assumes stationarity of species–environment relationships across time; this assumption is broadly supported by the low MESS extrapolation fraction (0.11% of pixels per scenario) which may not hold if monsoon dynamics shift non-linearly. Furthermore, the models do not incorporate biotic interactions, dispersal dynamics, or land-use change trajectories, all of which could substantially alter realised future distributions relative to pure climatic envelope projections. Finally, the ensemble lacks a direct out-of-fold evaluation row, preventing reporting of an overall ensemble AUC; individual algorithm performance metrics provide the basis for inference regarding ensemble skill but cannot substitute for direct ensemble evaluation.

5. Conclusions

This study presents the first nationally comprehensive ensemble species distribution model for Asian Elephant in Bhutan, integrating true-absence field survey data, CMIP6 multi-GCM projections, and spatially blocked cross-validation to identify critical climate refugia. The findings demonstrate that BIO18 is the dominant predictor across three of the four algorithms. Together with driest-month precipitation (BIO14), these variables define a subtropical moisture envelope that concentrates elephant habitat within the southern foothills. However, a severe gap in PA network remains evident; of the 4,649 km² of currently suitable habitat (14.1% of Bhutan), 74.1% (3,442 km²) lies outside the formal PA network, reflecting a historical PA placement bias toward high-elevation terrain.

While the models project relative climatic stability with long-term gains of up to +19.1% by the end of the century, this aggregate stability masks a committed near-term contraction of -6.1%

under the SSP5-8.5 scenario by 2050. This contraction is expected to elevate population pressure on remaining refugia during the critical 2021–2050 window. Furthermore, 4,160 km² identified as core climate refugia remain 53.6% unprotected, suggesting that securing or co-managing the remaining 2,230 km^2 is the single highest-leverage conservation action available. This urgency is compounded by a structurally inevitable escalation in conflict, with mean human–elephant conflict (HEC) risk projected to increase by 35.9% (0.103 → 0.140) by 2100. Because these risk trajectories are validated against 152 confirmed incidents, conflict management must be calibrated to future projections rather than contemporary baselines.

These findings support a multi-pronged approach centered on the southern belt. As 53.6% of core refugia lie outside the protected area network, biological corridor protection should be extended to encompass the unprotected 2,230 km² of core refugia, representing the highest-leverage conservation action. Given that 37.1% of non-protected land in the southern belt remains suitable, community-managed OECMs in Samdrup Jongkhar, Pemagatshel, and Sarpang should be prioritised under the GBF Target 3 framework. With mean human–elephant conflict risk projected to increase by 35.9% by 2100, mitigation infrastructure must be scaled in proportion to projected future risk rather than current levels. Finally, climate refugia should be integrated into Bhutan's Protected Area Management Plans and National Human–Wildlife Conflict Strategy to support long-term population persistence under climate change.

Acknowledgements

The authors thank the Department of Forests and Park Services (DoFPS), for providing occurrence data, protected area boundaries, and human–elephant conflict (HEC) records. The BhutanBioClims dataset (Dorji et al., 2024), developed by the Commonwealth Scientific and Industrial Research Organisation (CSIRO), was used to derive high-resolution bioclimatic variables for Bhutan. Access to Dynamic World and MODIS vegetation index datasets was facilitated through Google Earth Engine.

Author Contributions

Wangdi: Conceptualisation, Methodology, Software, Formal analysis, Visualisation, Investigation, Data Curation, Writing Original Draft. **Laxmi Sagar:** Resources, Investigation, Validation, Writing Review and Editing.

Conflict of Interest

The authors declare no conflict of interest.

Funding

This research received no external funding. The study was conducted as part of institutional research activities supported by the Department of Forests and Park Services (DoFPS), Royal Government of Bhutan.

Data Availability

Pipeline code, run configuration, and all tabular outputs are archived in the project repository in GitHub upon acceptance. Occurrence data are available from the Department of Forests and Park Services (DoFPS), upon reasonable request and subject to data-sharing agreements and national data governance policies. The BhutanBioClims dataset (Dorji et al., 2024) was used to derive high-resolution bioclimatic variables and is accessible via its DOI

(https://doi.org/10.25919/d8n7-5a07). Dynamic World land-cover data and MODIS vegetation index datasets are accessible via Google Earth Engine.

References

Araújo, M.B., & New, M. (2007). Ensemble forecasting of species distributions. *Trends in Ecology & Evolution*, 22(1), 42–47.

Barua, M., Bhagwat, S.A., & Jadhav, S. (2013). The hidden dimensions of human–wildlife conflict: health impacts, opportunity and transaction costs. *Biological Conservation*, 157, 309–316.

Breiman, L. (2001). Random forests. *Machine Learning*, 45(1), 5–32.

Brown, C.F., Brumby, S.P., Guzder-Williams, B., Birch, T., Hyde, S.B., Mazzariello, J., … & Tait, A.M. (2022). Dynamic World, near real-time global 10 m land use land cover mapping. *Scientific Data*, 9(1), 251.

Campos-Arceiz, A., & Blake, S. (2011). Megagardeners of the forest — the role of elephants in seed dispersal. *Acta Oecologica*, 37(6), 542–553.

Chen, I.C., Hill, J.K., Ohlemüller, R., Roy, D.B., & Thomas, C.D. (2011). Rapid range shifts of species associated with high levels of climate warming. *Science*, 333(6045), 1024–1026.

Choudhury, A., Lahiri Choudhury, D.K., Desai, A., Duckworth, J.W., Easa, P.S., Johnsingh, A.J.T., … & Wikramanayake, E. (2008). *Elephas maximus*. IUCN Red List of Threatened Species 2008: e.T7140A12828813.

de Silva, S., & Leimgruber, P. (2019). Demographic tipping points as early indicators of vulnerability for slow-breeding megafaunal populations. *Frontiers in Ecology and Evolution*, 7, 171.

DoFPS (2020). *National Survey of Elephants in Bhutan*. Department of Forests and Park Services, Royal Government of Bhutan, Thimphu.

Dorji, S., Stewart, S., Shabbir, A., Bajwa, A., Aziz, A., & Adkins, S. (2025). Comparative analysis of mechanistic and correlative models for global and Bhutan-specific suitability of parthenium weed and vulnerability of agriculture in Bhutan. *Plants*, *14*(1), Article 83.

Elith, J., Graham, C.H., Anderson, R.P., Dudík, M., Ferrier, S., Guisan, A., … & Zimmermann, N.E. (2006). Novel methods improve prediction of species' distributions from occurrence data. *Ecography*, 29(2), 129–151.

Elith, J., Leathwick, J.R., & Hastie, T. (2008). A working guide to boosted regression trees. *Journal of Animal Ecology*, 77(4), 802–813.

Elith, J., & Leathwick, J.R. (2009). Species distribution models: ecological explanation and prediction across space and time. *Annual Review of Ecology, Evolution, and Systematics*, 40, 677–697.

Elith, J., Kearney, M., & Phillips, S. (2010). The art of modelling range-shifting species. *Methods in Ecology and Evolution*, 1(4), 330–342.

Fernando, P., Wikramanayake, E., Weerakoon, D., Jayasinghe, L.K.A., Gunawardene, M., & Janaka, H.K. (2012). Perceptions and patterns of human–elephant conflict in old and new settlements in Sri Lanka: insights for mitigation and management. *Biodiversity and Conservation*, 14(10), 2465–2481.

Franklin, J. (2010). *Mapping Species Distributions: Spatial Inference and Prediction*. Cambridge University Press.

Friedman, J.H. (2001). Greedy function approximation: a gradient boosting machine. *Annals of Statistics*, 29(5), 1189–1232.

Guisan, A., Edwards, T.C., & Hastie, T. (2002). Generalised linear and generalised additive models in studies of species distributions: setting the scene. *Ecological Modelling*, 157(2–3), 89–100.

Hao, T., Elith, J., Guillera-Arroita, G., & Lahoz-Monfort, J.J. (2020). Testing whether ensemble modelling is advantageous for maximising predictive performance of species distribution models. *Ecography*, 43(4), 549–558.

Hirzel, A.H., & Le Lay, G. (2008). Habitat suitability modelling and niche theory. *Journal of Applied Ecology*, 45(5), 1372–1381.

Hirzel, A.H., Le Lay, G., Helfer, V., Randin, C., & Guisan, A. (2006). Evaluating the ability of habitat suitability models to predict species presences. *Ecological Modelling*, 199(2), 142–152.

Joppa, L.N., & Pfaff, A. (2009). High and far: biases in the location of protected areas. *PLoS ONE*, 4(12), e8273.

Keppel, G., Van Niel, K.P., Wardell-Johnson, G.W., Yates, C.J., Byrne, M., Mucina, L., … & Franklin, S.E. (2012). Refugia: identifying and understanding safe havens for biodiversity under climate change. *Global Ecology and Biogeography*, 21(4), 393–404.

Leimgruber, P., Gagnon, J.B., Wemmer, C., Kelly, D.S., Songer, M.A., & Selig, E.R. (2003). Fragmentation of Asia's remaining wildlands: implications for Asian elephant conservation. *Animal Conservation*, 6(4), 347–359.

Matthews, H.D., & Caldeira, K. (2008). Stabilizing climate requires near-zero emissions. *Geophysical Research Letters*, 35(4), L04705.

Merow, C., Smith, M.J., & Silander, J.A. (2013). A practical guide to MaxEnt for modeling species' distributions: what it does, and why inputs and settings matter. *Ecography*, 36(10), 1058–1069.

Mondal, I., Thakur, S., Ghosh, P., & Bandyopadhyay, J. (2023). Modelling spatial distribution of Asian elephant (*Elephas maximus*) in a fragmented landscape of sub-Himalayan Bengal, India. *Ecological Informatics*, 73, 101930.

Morelli, T.L., Barrows, C.W., Ramirez, A.R., Cartwright, J.M., Ackerly, D.D., Eaves, T.D., … & Tague, C.L. (2020). Climate-change refugia: biodiversity in the slow lane. *Frontiers in Ecology and the Environment*, 18(5), 228–234.

Phillips, S.J., Anderson, R.P., & Schapire, R.E. (2006). Maximum entropy modeling of species geographic distributions. *Ecological Modelling*, 190(3–4), 231–259.

Phillips, S.J., Anderson, R.P., Dudík, M., Schapire, R.E., & Blair, M.E. (2017). Opening the black box: an open-source release of Maxent. *Ecography*, 40(7), 887–893.

R Core Team (2024). *R: A Language and Environment for Statistical Computing*. R Foundation for Statistical Computing, Vienna.

Roberts, D.R., Bahn, V., Ciuti, S., Boyce, M.S., Elith, J., Guillera-Arroita, G., … & Dormann, C.F. (2017). Cross-validation strategies for data with temporal, spatial, hierarchical, or phylogenetic structure. *Ecography*, 40(8), 913–929.

Sanderson, B.M., Knutti, R., & Caldwell, P. (2015). A representative democracy to reduce interdependency in a multimodel ensemble. *Journal of Climate*, 28(13), 5171–5194.

Sukumar, R. (1989). *The Asian Elephant: Ecology and Management*. Cambridge University Press.

Sukumar, R. (2006). A brief review of the status, distribution and biology of wild Asian elephants. *International Zoo Yearbook*, 40(1), 1–8.

Telwala, Y., Brook, B.W., Manish, K., & Pandit, M.K. (2013). Climate-induced elevational range shifts and increase in plant species richness in a Himalayan biodiversity epicentre. *PLoS ONE*, 8(2), e57103.

Valavi, R., Elith, J., Lafond, J.J., & Guillera-Arroita, G. (2019). blockCV: an R package for generating spatially or environmentally separated folds for k-fold cross-validation of species distribution models. *Methods in Ecology and Evolution*, 10(2), 225–232.

Venter, O., Magrach, A., Outram, N., Klein, C.J., Possingham, H.P., Di Marco, M., & Watson, J.E.M. (2018). Bias in protected-area location and its effects on long-term aspirations of biodiversity conventions. *Conservation Biology*, 32(1), 127–134.

Wang, S.W., & Macdonald, D.W. (2006). Livestock predation by carnivores in Jigme Singye Wangchuck National Park, Bhutan. *Biological Conservation*, 129(4), 558–565.

Wangchuk, T. (2004). Predator-prey dynamics and problems in Bhutan. *Journal of the Bhutan Ecological Society*, 1, 55–63.

Wildlife Conservation Society / CIESIN (2005). *Last of the Wild Project, Version 2 (LWP-2): Global Human Footprint Dataset (Geographic)*. NASA Socioeconomic Data and Applications Center (SEDAC), Palisades, NY.

Williams, A.C., Johnsingh, A.J.T., & Krausman, P.R. (2020). Human–elephant conflicts in Rajaji-Corbett National Parks, northwestern India. *Wildlife Society Bulletin*, 49(3), 461–468.

Zurell, D., Franklin, J., König, C., Bouchet, P.J., Dormann, C.F., Elith, J., … & Merow, C. (2020). A standard protocol for reporting species distribution models. *Ecography*, 43(9), 1261–1277.